ROYAL SOCIETY
OF CHEMISTRY

PAPER

Check for updates

SD aromaticity index: a new assessment of aromaticity based on Ramsey spin dipolar contribution to NMR spin–spin coupling constants

M. Natalia C. Zarycz, [ID] *[a] M. Ayelén Schiel, [ID] [a] Héctor A. Baldoni [ID] [b] and Ricardo D. Enriz [ID] [a]

Aromaticity remains one of the most fundamental yet elusive concepts in chemistry, as no single observable can directly quantify it. In this work, we introduce the spin–dipolar aromaticity index (SDAI), a new descriptor based on the spin–dipolar (SD) contribution to one-bond NMR spin–spin coupling constants. Beyond providing an additional numerical index, SDAI unveils a direct physical manifestation of aromaticity through the magnetic interaction between nuclear spins mediated by delocalized π-electrons. Within the framework of density functional theory (DFT), we analyzed the behavior of the SD term across a representative series of aromatic, nonaromatic, and antiaromatic molecules, including heterocycles, substituted benzenes, fulvenes, and polycyclic hydrocarbons. The calculations show that in aromatic systems, the SD contribution to one bond coupling ($^1J^{SD}$) exhibits nearly uniform values—close to those of benzene—reflecting a collective and homogeneous spin-polarization response of the π-system. In contrast, nonaromatic and antiaromatic compounds display irregular $^1J^{SD}$ patterns, with large bond-to-bond variations that reflect localized π-electron distributions. This magnetic uniformity is therefore a necessary but not sufficient condition for aromaticity: only when the resulting $^1J^{SD}$ values remain comparable to benzene's does genuine aromatic character arise. The aromaticity trends obtained from SDAI closely reproduce those given by electronic and energetic descriptors such as HOMA, PDI, and FLU. Moreover, in molecules where magnetic and electronic criteria diverge, SDAI follows the latter, confirming its consistency with descriptors governed by π-electron delocalization. SDAI thus provides a physically grounded and computationally accessible approach to quantify aromaticity.

1. Introduction

Aromatic compounds, including cyclic hydrocarbons and their heterocyclic analogs, are essential in chemical research and applications, from drug design and polymer synthesis to materials for organic electronics, as well as in biological systems such as DNA and coenzymes.[1–10] This importance has driven over a century of studies aimed at understanding the factors governing their chemical and physical properties.[5,11–20]

Despite extensive research, the definition and quantification of aromaticity remain contentious.[16,21–23] Aromaticity cannot be defined unequivocally, as there is no physical observable that allows its direct measurement. This chemical unicorn[24] is inferred from properties that characterize aromatic systems.[5,14,15,17,18,25] A molecule is generally considered aromatic when it exhibits delocalized π-electrons, enhanced energetic stability relative to acyclic analogs, bond-length equalization, diamagnetic ring currents under an external magnetic field, and a tendency toward substitution rather than addition reactions. Although these criteria form a useful framework, they cannot always be consistently applied, and no single property can universally define aromaticity.[5,26] Indeed, different indices based on these properties can yield contradictory results.[15] This is often attributed to the multidimensional nature of aromaticity, which implies that not all related properties are equally affected.[27] While this explanation may be reasonable in some instances, invoking multidimensionality cannot justify cases where certain aromaticity criteria fail or the indices are applied beyond their range of validity.[28,29]

[a] Facultad de Química, Bioquímica y Farmacia, Instituto Multidisciplinario de Investigaciones Biológicas de San Luis (IMIBIO-SL), CONICET, Universidad Nacional de San Luis, 5700 San Luis, Argentina. E-mail: mnzarycz@gmail.com

[b] Facultad de Química, Bioquímica y Farmacia, Instituto de Matemáticas Aplicadas (IMASL), CONICET, Universidad Nacional de San Luis, Italia 1556, San Luis, 5700, Argentina

Since typical aromatic and antiaromatic compounds exhibit diatropic and paratropic ring currents, respectively, under an external magnetic field, magnetic properties are widely used to characterize aromaticity. Methods based on this criterion include magnetic susceptibility anisotropy,[30–32] magnetic susceptibility exaltation,[33–35] proton NMR chemical shifts,[36,37] interatomic magnetizabilities,[38] nucleus-independent chemical shifts (NICS),[13] and magnetically induced current density (MICD) plots.[39–49] Despite its limitations, NICS remains the most widely used approach. Its main drawback is that it measures shielding/deshielding at a single point without revealing the current sources.[14,28] Consequently, a NICS value may arise from local atomic currents, adjacent rings, or the ring of interest, leading to misinterpretations as reported for polycyclic hydrocarbons,[28,50,51] hydrogen-bonded clusters,[52] and all-metal aromatics.[53,54] The isotropic NICS(0) and NICS(1) indices give misleading results.[14] For monocyclic systems, the most reliable NICS variants are NICS(1)$_{zz}$ and NICS(1)$_{\pi zz}$, though they are unsuitable for polycyclic systems. Although these indices better characterize π-electron currents, they should be combined with MICD plots to confirm that the NICS values originate from the ring current rather than from other current–density features.[14,28] The magnetic criterion faces limitations beyond the ill-defined nature of some derived indices. For example, there are reports of systems with diatropic currents that are not aromatic by energetic or electronic criteria,[29,55] and cases of radical ions of benzene and heterocycles exhibiting paratropic currents despite cyclic conjugation.[56] These observations have led some authors to question its reliability,[29] while others propose distinguishing magnetic aromaticity (based on currents) from intrinsic aromaticity (defined by energetic, electronic, and geometric criteria).[55,57] Turning to the geometric criterion, Hiberty, Shaik, and co-workers[58] attributed bond equalization in benzene to an anti-distortive σ-electron effect, although later studies revealed an additional contribution from anti-distortive cyclic delocalization energy of the π system.[59,60] The energetic criterion is fundamental for characterizing aromaticity, but its use is hindered by the need for an appropriate reference system to isolate stabilization from other energy effects.[18] The criterion of cyclic π-electron delocalization is also intrinsic; indeed, several studies have established a direct relationship between the energetic and electronic criteria.[12,29,55,61] Nevertheless, as emphasized previously,[28] all aromaticity indices have inherent limitations, and overlooking them can lead to misapplication and erroneous conclusions. Therefore, a multifaceted approach using indices based on different physical properties is essential for reliably evaluating the aromatic character of a system.[16]

Besides magnetic-based indices, the most commonly used aromaticity measures include the aromatic stabilization energy (ASE),[18] an energy-based measure; the harmonic oscillator model of aromaticity (HOMA),[25] a geometry-based indicator; and electron density-based indices such as the *para*-delocalization index (PDI),[62] the aromatic fluctuation index (FLU)[63] and the electron density of delocalized bonds (EDDB).[64] A recent and promising contribution to this last category is the set of six new descriptors introduced by Borges Jr. and co-workers, derived from the analysis of delocalized electron density using Stone's distributed multipole analysis (DMA).[65]

NMR indirect spin–spin coupling constants (*J*-couplings) are highly sensitive probes of electronic structure, and their accurate prediction is now feasible with modern quantum-chemical methods.[66–70] *J*-Coupling depends on σ or π chemical bond character between the coupled nuclei. Such dependency can be analyzed by using the classic Ramsey theory.[71] Thus, the Fermi contact (FC) mechanism dominates in σ frameworks; whereas spin–dipolar (SD) and paramagnetic spin–orbital (PSO) terms reflect the presence of π electrons.[72–76] Although the role of these non-contact terms in conjugated C–C bonds remains partially unresolved, long-range couplings are known to require π-conjugation, where SD and PSO can outweigh FC.[75–77] Our recent study on *o*-hydroxyaryl Schiff bases[77] showed that π-delocalization in the chelate ring produces significant SD and PSO contributions to ^{2h}J(O–N), affecting the tautomeric equilibrium and corroborating resonance-assisted hydrogen bonding. Moreover, the variation of the SD term with d(NH) closely follows the changes in the PDI, providing novel evidence for a direct relationship between the SD mechanism and π-electron delocalization in cyclic systems.

Since π-electron delocalization in cyclic systems is generally considered the main cause of their aromatic character and considering that the spin–dipolar contribution to *J*-coupling (J^{SD}) is a highly sensitive probe of the π-electron distribution, analyzing how aromaticity affects this term provides a valuable means to gain physical insight into this elusive property. In fact, we found that the SD contribution to the one-bond *J*-coupling between nuclei M and N, $^1J^{SD}$(M,N), exhibits distinctive behavior in aromatic systems: all bonds show nearly identical values, reflecting a homogeneous delocalization of the π-electrons. For instance, at the B3LYP/cc-pVTZ level, in benzene every $^1J^{SD}$(C,C) coupling is 1.27 Hz, while in other 6π-electron aromatic systems such as $C_7H_7^+$ and $C_8H_8^{2+}$ the values decrease slightly to 1.13 and 1.08 Hz, respectively, indicating a reduction of aromatic character with increasing ring size. By contrast, in non-aromatic and antiaromatic systems the $^1J^{SD}$(C,C) values are not uniform, often around 4 Hz or higher for localized double bonds, directly revealing the lack of π-electron delocalization. Thus, just as bond-length alternation evidences electronic localization, the dispersion of $^1J^{SD}$(M,N) values constitutes a direct physical manifestation of how the degree of aromaticity modulates the underlying spin interactions responsible for the SD mechanism.

Given that the definition and physical origin of aromaticity remain debated and not fully established, requiring a multifaceted description, several authors have emphasized the need for new descriptors from complementary perspectives.[16,21,22,78] Within this context, $^1J^{SD}$(M,N) emerges as a genuine quantum-physical property that provides new insight into aromaticity by directly probing the π-electron distribution along bonds. The main goal of this study is therefore not merely to propose another index, but to establish a physically grounded descriptor—here termed the spin–dipolar aromaticity index (SDAI)—which formalizes the distinctive behavior of $^1J^{SD}$(M,N)

This journal is © the Owner Societies 2025

Phys. Chem. Chem. Phys., 2025, **27**, 22974–22989 | **22975**

values: uniform and close to 1.2 Hz in aromatic compounds, and heterogeneous and larger for localized double bonds in non-aromatic or antiaromatic ones. By doing so, this index provides a direct and measurable connection between π-electron delocalization in aromatic/antiaromatic systems and the underlying spin interactions responsible for the spin–dipolar mechanism. Furthermore, we aim to clarify whether SDAI follows more closely the predictions of magnetic or electronic descriptors in molecules where these criteria diverge.[29,55] To validate this approach, we applied SDAI to a representative set of cyclic and polycyclic hydrocarbons and their heteroatomic analogues with well-established aromaticity trends, and we compared the results with those from established indices such as HOMA, PDI, FLU, and NICS.

2. Theoretical models

2.1 Origin of NMR *J*-couplings

This section briefly outlines the physical mechanisms responsible for *J*-couplings observed in NMR spectra of solutions or gases. While all electronic mechanisms are mentioned, particular focus is placed on those dependent on electron spin. Detailed descriptions of the underlying theory and its quantum-chemical determination are available in textbooks and reviews.[66–69]

Within a non-relativistic framework, Ramsey developed the theory of *J*-couplings, proposing that nuclear spins interact *via* electrons located along the coupling pathway.[71] The isotropic *J*-coupling between nuclei K and L is given by the sum of four contributions:

$$J_{KL} = J_{KL}^{DSO} + J_{KL}^{PSO} + J_{KL}^{FC} + J_{KL}^{SD} \qquad (1)$$

These terms correspond to the diamagnetic spin–orbital (DSO), paramagnetic spin–orbital (PSO), Fermi-contact (FC), and spin-dipolar (SD) mechanisms.

The J_{KL}^{DSO} term is an expectation value of the ground-state wave function and is straightforward to calculate. The PSO, FC, and SD terms were originally formulated as a sum-over-states, requiring knowledge of all singlet (PSO) or triplet (FC, SD) excited states. Although this formulation describes the underlying physics, it is not suitable for computation. In practice, *J*-couplings are typically evaluated using linear response methods.[79,80]

Ramsey's formulation distinguishes two types of transmission mechanisms. The first, independent of electron spin, involves interactions between nuclear magnetic fields and electron orbital motion (DSO and PSO). The second, dependent on electron spin, arises from interactions between nuclear magnetic moments and electron spins (FC and SD). In essence, *J*-coupling occurs when the magnetic field of one nucleus perturbs the surrounding electron cloud, transmitting this disturbance through the electronic system and inducing a secondary magnetic field at the position of the other nucleus. The latter nucleus then interacts with this induced field.

For spin-dependent interactions, one nucleus induces a local polarization of electron spins, leading to a relative excess or deficit of α electrons compared to β electrons. When this polarization occurs at the nuclear positions, the interaction is governed by the FC mechanism. Polarization in the extended dipolar field outside the nuclei is described by the SD term. Although this work is restricted to closed-shell systems, local regions of non-zero spin density (the difference between α- and β-electron densities) may arise. Positive and negative contributions, however, compensate globally so that the total number of α and β electrons remains equal.

The FC contribution arises from nucleus–electron interactions at the nuclear contact surface, involving s-orbitals. It is therefore mainly transmitted through the σ-bond framework and dominates *J*-couplings in saturated molecules. The SD term originates from interactions away from nuclei and is primarily transmitted through π-systems, becoming significant in unsaturated molecules. Among the spin-independent terms, the DSO contribution is often negligible, though exceptions exist.[81] In contrast, the PSO term is typically significant when coupled atoms are linked through π-systems or possess lone pairs.

3. Computational details

All calculations of NMR spectroscopic parameters and geometry optimizations were performed using DFT[82] methodology with the Gaussian 16 program package.[83] The geometries were optimized using the B3LYP-D3(BJ)[84–86] functional with the 6-311++G(d,p) basis set.[87]

J-Couplings were calculated using the B3LYP,[84,88] PBE,[89] and B3P86[88,90] functionals combined with the aug-cc-pVTZ-J,[91] ccJ-pVTZ,[92] and cc-pVTZ[93] basis sets.

Nuclear magnetic shielding constants for the NICS indices were obtained at the B3LYP/aug-cc-pVTZ level using the gauge-independent atomic orbital (GIAO) method.[94,95]

The optimized geometries were used to compute wavefunctions at the Hartree Fock (HF) level with the cc-pVTZ basis set using Gaussian 16, and the resulting data were employed to calculate delocalization indices (DIs)[62] within the quantum theory of atoms in molecules (QTAIM)[96] with the Multiwfn software.[97]

Previous studies have[62] shown that DI values for closed-shell systems calculated at the HF level are accurate compared with those from configuration interaction with singles and doubles excitations (CISD), despite a moderate overestimation. Since the qualitative trends are preserved and CISD calculations are computationally prohibitive for the systems studied here, the HF level represents a suitable choice for obtaining reliable DI values.

The geometries of compounds **A17–A21** were taken from previous works.[29,55] For compounds **A19–A21**, which are in their lowest triplet state, *J*-coupling calculations were performed at the UB3LYP/cc-pVTZ level.

4. Results and discussion

4.1 Assessment of Ramsey's terms of carbon–carbon coupling constants as probes of conjugation and aromaticity

If a molecular property is to function as the basis for an aromaticity index, it must distinguish between saturated and

22976 | *Phys. Chem. Chem. Phys.*, 2025, **27**, 22974–22989

This journal is © the Owner Societies 2025

unsaturated compounds. Among the latter, its value should vary between systems with conjugated and non-conjugated double bonds, as well as between aromatic, non-aromatic, and antiaromatic frameworks.

In this section, we evaluate the behavior of the SD (J^{SD}), PSO (J^{PSO}) and FC (J^{FC}) contributions to J-coupling with the aim of verifying whether any of them meets the requirements to define an aromaticity index.

4.1.1 DFT functional and basis set selection. A key requirement for any theoretical approximation aimed at assessing Ramsey's contributions to J-coupling is its ability to reliably reproduce experimental data. Previous studies have shown that DFT methods provide accurate carbon–carbon J-coupling constants ($J(C,C)$) in close agreement with experiment.[70,98] Suardiaz et al. reported that B3LYP, PBE, and B3P86 combined with the aug-cc-pVTZ-J basis set reproduce experimental values with excellent accuracy for molecules with different carbon hybridizations.[99] This basis set was optimized for an improved description of the FC term by including tight s-functions on the coupled nuclei.[91]

To properly describe the SD and PSO terms, however, additional tight d- and p-functions are required. The ccJ-pVTZ basis set, optimized by Jensen and co-workers for J-coupling calculations, fulfills this requirement.[92] While it has shown excellent performance with coupled-cluster and SOPPA-family methods,[100] it had not been tested with the B3LYP, B3P86, and PBE functionals for molecules encompassing diverse carbon hybridizations, such as those in Fig. 1.

To evaluate the quality of the chosen functionals and basis sets, we selected 21 molecules (63 $J(C,C)$ values) covering sp^3–sp^3, sp^3–sp^2, and sp^2–sp^2 bond types (see Fig. S1, SI), with experimental values ranging from -2 to 75 Hz (Table S1, SI). Linear regression analyses between calculated and experimental data show excellent agreement (Fig. 2), yielding coefficients $R^2 > 0.99$ for all functional/basis-set combinations. The mean absolute errors (MAEs) were similarly low, ranging from 1.80 to 2.50 Hz (Table S2, SI). The B3P86/aug-cc-pVTZ-J combination provided the lowest MAE (1.80 Hz), but the differences among methods were minor. For instance, switching to the ccJ-pVTZ basis set altered the MAEs by less than 0.23 Hz. These results confirm that both ccJ-pVTZ and aug-cc-pVTZ-J reproduce experimental J-couplings with comparable and reliable accuracy.
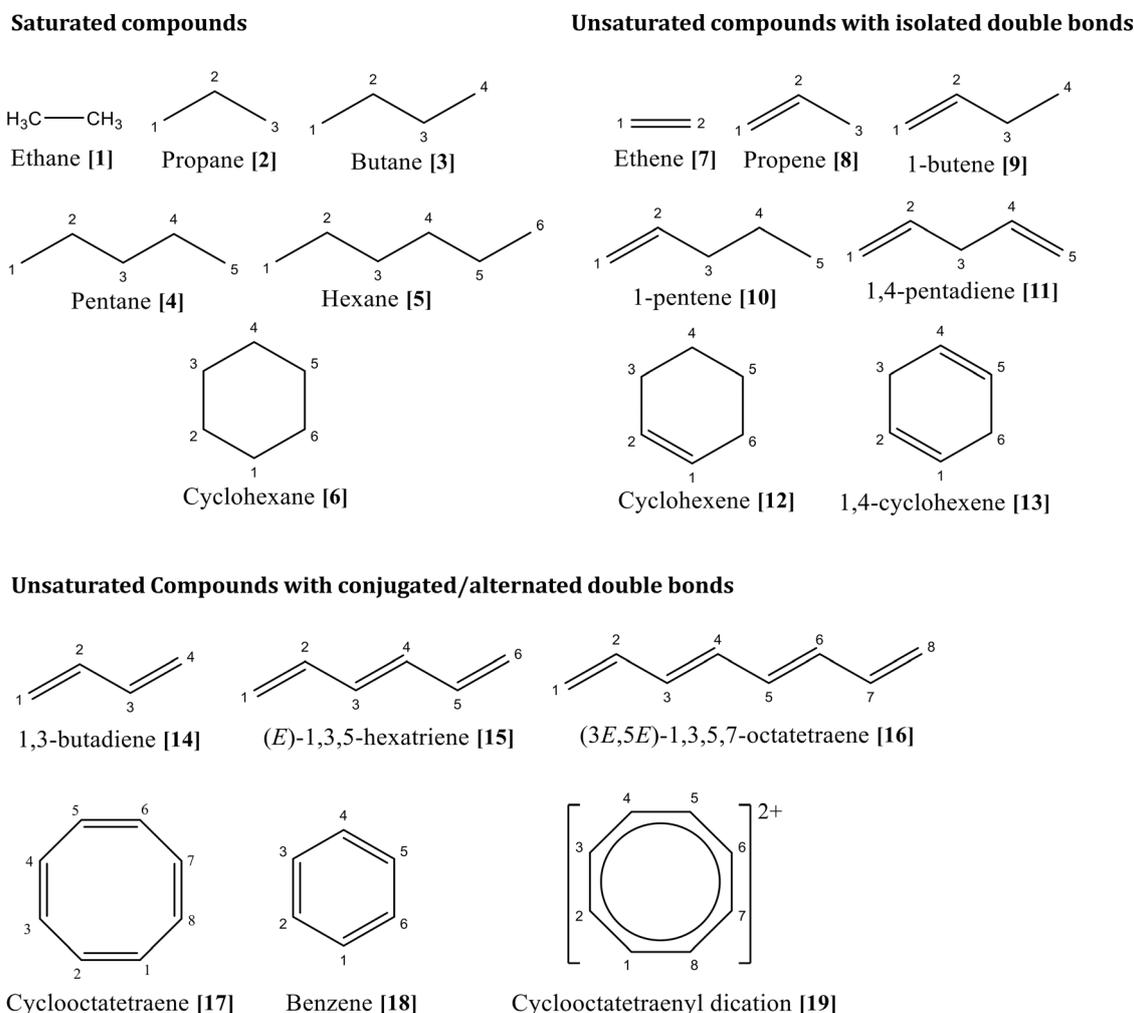

Fig. 1 Schematic structures of saturated and unsaturated compounds used to assess the behavior of the J-coupling Ramsey terms.
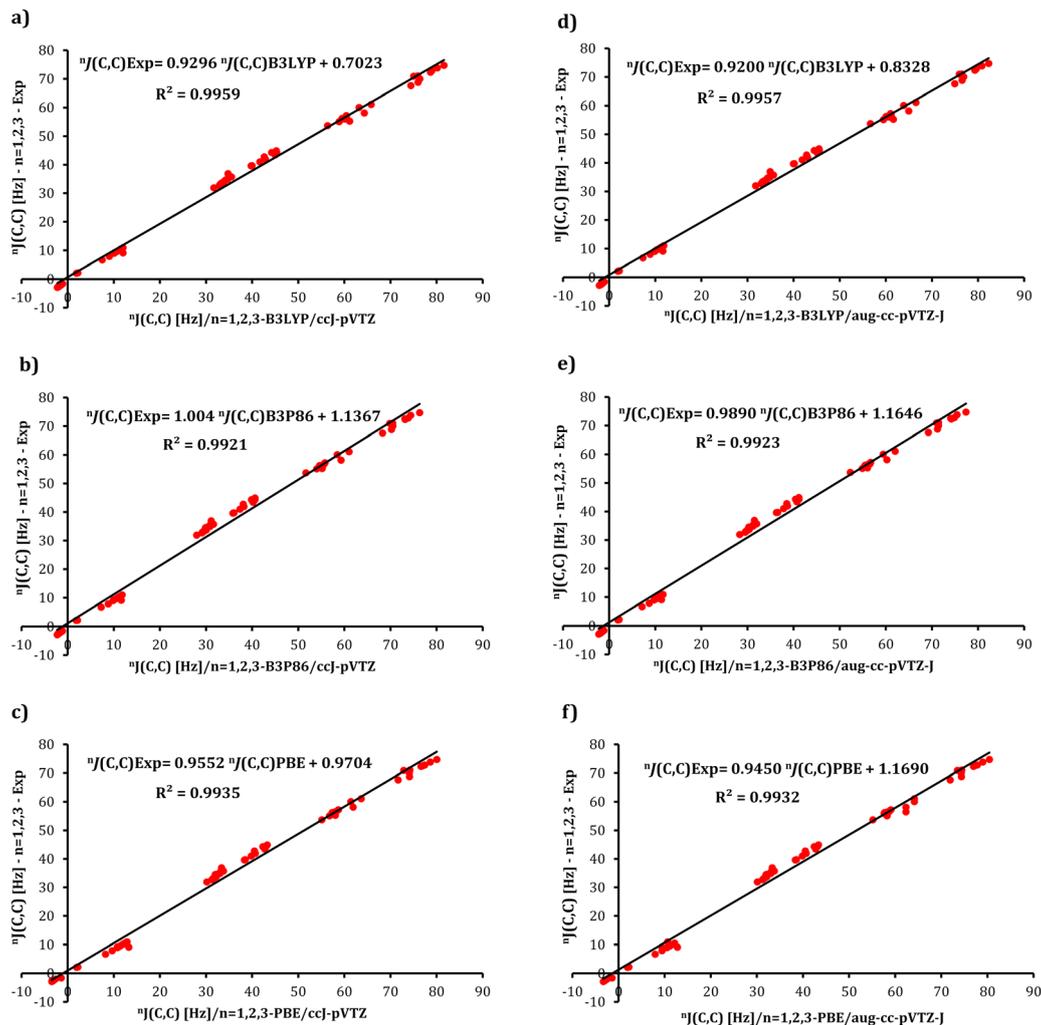
This journal is © the Owner Societies 2025

Phys. Chem. Chem. Phys., 2025, **27**, 22974–22989 | **22977**

Fig. 2 Relationship between experimental ^{n}J(C,C) values (n = 1, 2, 3) and those calculated at the following levels of approximation: (a) B3LYP/ccJ-pVTZ, (b) B3P86/ccJ-pVTZ, (c) PBE/ccJ-pVTZ, (d) B3LYP/aug-cc-pVTZ-J, (e) B3P86/aug-cc-pVTZ-J, and (f) PBE/aug-cc-pVTZ-J, for the selected compounds (Fig. S1, SI).

A direct comparison of the two basis sets across all three functionals (Fig. S2, SI) further supports their equivalence. The linear correlations for all functionals show slopes close to unity, intercepts near zero, and R^2 values of 1.000 for B3LYP and B3P86 and 0.999 for PBE. Given this comparable accuracy, and since ccJ-pVTZ is smaller and computationally more efficient, we selected the B3LYP/ccJ-pVTZ level of theory for the subsequent calculations of Ramsey terms in the molecular systems of Fig. 1.

4.1.2 Analysis of Ramsey terms behavior. Table 1 reports the total values and the FC, SD, and PSO contributions to the carbon–carbon J-couplings of the selected compounds (Fig. 1). The DSO term is omitted because it is negligible in all cases. Our aim is to compare the behavior of these Ramsey contributions across one or more bonds in three groups of compounds: saturated; with isolated double bonds; and with conjugated or alternating double bonds, including aromatic species.

Across all compounds, the one-bond coupling, ^{1}J(C,C), is the largest. The ^{1}J(C,C) magnitude is primarily determined by the

FC contribution, which depends on the hybridization of the coupled atoms and on the presence of a π bond; J^{SD}(C,C) and J^{PSO}(C,C) often provide important corrections depending on the bonding environment. This trend is in line with previous works.[70,74,98]

4.1.2.1 Saturated compounds. For saturated compounds (**1–6**), ^{1}J(C,C) values lie around 33 Hz (see Table 1). Two-bond couplings are nearly zero in linear systems but reach ≈ -1.4 Hz in cyclohexane; couplings beyond three bonds are negligible. For couplings beyond one bond, the SD and PSO contributions are practically zero. Thus, the through-space mechanism observed for ^{3}J(C,C) in these saturated systems is attributable exclusively to the FC contribution.

4.1.2.2 Compounds with isolated double bonds. For compounds **7–13**, ^{1}J(C,C) across a double bond is ≈ 74–77 Hz, whereas for σ sp³–sp² ^{1}J(C,C) values are ≈ 40–44 Hz and for σ sp³–sp³ ≈ 32–35 Hz. Two-bond couplings are small (≈ -1.8

22978 | *Phys. Chem. Chem. Phys.*, 2025, **27**, 22974–22989

This journal is © the Owner Societies 2025

Table 1 Total C–C coupling constant and their Ramsey contribution (in Hz) for selected compound (see Fig. 1) computed at B3LYP/ccJ-pVTZ level

Comp.		FC	SD	PSO	Tot	Comp.		FC	SD	PSO	Tot
1	^1J(C1,C2)	32.91	1.16	0.00	34.19	**12**	^1J(C1,C2)	81.83	3.88	−10.14	75.76
2	^1J(C1,C2)	33.09	1.16	−0.26	34.15		^1J(C2,C3)	40.71	0.87	−1.27	40.53
	^2J(C1,C3)	−0.11	−0.05	−0.22	−0.40		^1J(C3,C4)	32.38	1.25	−0.27	33.58
3	^1J(C1,C2)	33.32	1.17	−0.27	34.38		^1J(C4,C5)	31.40	1.20	−0.43	32.39
	^1J(C2,C3)	33.22	1.16	−0.57	34.01		^2J(C1,C3)	−0.29	0.01	−0.37	−0.67
	^2J(C1,C3)	0.27	−0.05	−0.24	−0.03		^2J(C2,C4)	−1.53	−0.03	−0.12	−1.66
	^3J(C1,C4)	6.42	0.03	0.01	6.40		^2J(C3,C5)	−1.30	−0.05	−0.12	−1.44
4	^1J(C1,C2)	33.36	1.17	−0.26	34.43		^3J(C1,C4)	6.20	−0.02	−0.14	6.06
	^1J(C2,C3)	33.47	1.16	−0.57	34.26		^3J(C3,C6)	3.89	−0.01	−0.09	3.79
	^1J(C3,C4)	33.50	1.16	−0.57	34.29	**13**	^1J(C1,C2)	82.85	3.96	−10.16	76.84
	^2J(C1,C3)	0.15	−0.05	−0.24	−0.15		^1J(C2,C3)	41.79	0.87	−1.28	41.61
	^2J(C2,C4)	0.61	−0.05	−0.25	0.32		^2J(C1,C3)	−0.49	0.00	−0.33	−0.84
	^3J(C1,C4)	6.16	0.04	0.00	6.14		^2J(C2,C4)	−1.89	−0.02	0.05	−1.83
	^4J(C1,C5)	0.34	−0.01	0.04	0.33		^3J(C1,C4)	8.04	0.05	−0.06	8.04
5	^1J(C1,C2)	33.35	1.17	−0.26	34.42		^3J(C3,C6)	7.46	0.00	−0.16	7.28
	^1J(C2,C3)	33.52	1.16	−0.57	34.32	**14**	^1J(C1,C2)	81.53	4.07	−9.77	75.96
	^1J(C3,C4)	33.74	1.16	−0.58	34.53		^1J(C2,C3)	57.80	1.38	−3.01	56.36
	^1J(C4,C5)	33.54	1.16	−0.57	34.34		^2J(C1,C3)	1.00	−1.57	0.10	−0.53
	^2J(C1,C3)	0.17	−0.05	−0.24	−0.13		^3J(C1,C4)	7.89	3.50	0.69	11.98
	^2J(C2,C4)	0.48	−0.05	−0.25	0.20	**15**	^1J(C1,C2)	81.51	4.18	−9.62	76.20
	^3J(C1,C4)	5.96	0.04	0.00	5.94		^1J(C2,C3)	61.01	1.61	−3.38	59.45
	^3J(C2,C5)	5.92	0.04	−0.01	5.90		^2J(C1,C3)	0.71	−2.28	0.14	−1.47
	^4J(C1,C5)	0.35	−0.01	0.04	0.34		^2J(C2,C4)	1.62	−1.56	−0.01	0.02
	^5J(C1,C6)	0.17	0.00	0.04	0.18		^3J(C1,C4)	8.13	3.66	0.68	12.40
6	^1J(C1,C2)	31.82	1.21	−0.40	32.85		^3J(C2,C5)	8.42	0.60	0.15	9.12
	^2J(C1,C3)	−1.23	−0.05	−0.17	−1.42		^4J(C1,C5)	−1.23	−1.12	0.03	−2.37
	^3J(C1,C4)	2.26	−0.01	−0.08	2.19		^5J(C1,C6)	1.42	2.39	−0.09	3.68
7	^1J(C1,C2)	80.53	4.03	−10.21	74.42	**16**	^1J(C1,C2)	81.55	4.27	−9.56	76.39
8	^1J(C1,C2)	82.20	4.21	−10.17	76.35		^1J(C2,C3)	61.80	1.78	−3.52	60.27
	^1J(C2,C3)	42.61	0.93	−0.82	42.87		^2J(C1,C3)	0.47	−2.74	0.16	−2.15
	^2J(C1,C3)	1.16	0.03	−0.33	0.79		^2J(C2,C4)	1.43	−1.59	−0.03	−0.22
9	^1J(C1,C2)	81.97	4.18	−10.18	76.09		^2J(C3,C5)	1.29	−2.28	0.02	−0.98
	^1J(C2,C3)	42.40	0.94	−1.04	42.49		^3J(C1,C4)	8.42	3.80	0.67	12.80
	^1J(C3,C4)	33.81	1.20	−0.15	35.02		^3J(C2,C5)	8.74	0.84	0.18	9.71
	^2J(C1,C3)	1.55	0.03	−0.31	1.22		^4J(C1,C5)	−1.55	−1.65	0.03	−3.22
	^2J(C2,C4)	0.06	0.00	−0.13	−0.06		^4J(C2,C6)	−1.57	−1.19	0.03	−2.77
	^3J(C1,C4)	5.53	0.02	0.14	5.61		^5J(C1,C6)	1.76	2.61	−0.10	4.22
10	^1J(C1,C2)	82.12	4.18	−10.19	76.24		^5J(C2,C7)	1.51	0.38	0.01	1.87
	^1J(C2,C3)	42.79	0.93	−1.07	42.86		^6J(C1,C7)	−1.17	−0.84	0.03	−2.01
	^1J(C3,C4)	33.90	1.19	−0.45	34.84		^7J(C1,C8)	1.08	1.92	0.05	3.03
	^1J(C4,C5)	33.57	1.16	−0.29	34.84	**17**	^1J(C1,C2)	84.97	4.12	−9.90	79.39
	^2J(C1,C3)	1.42	0.03	−0.32	1.08		^1J(C2,C3)	59.56	0.86	−2.19	58.45
	^2J(C2,C4)	0.58	0.00	−0.14	0.46		^2J(C1,C3)	−1.28	0.01	−0.11	−1.39
	^2J(C3,C5)	0.63	−0.05	−0.23	0.35		^3J(C1,C4)	4.07	−0.49	0.02	3.59
	^3J(C1,C4)	5.37	0.03	0.14	5.47		^3J(C2,C5)	4.03	−0.12	−0.07	3.86
	^3J(C2,C5)	7.15	0.04	0.02	7.16		^4J(C1,C5)	−2.38	0.10	0.01	−2.26
	^4J(C1,C5)	0.57	0.01	0.08	0.61	**18**	^1J(C1,C2)	65.05	1.38	−7.23	59.41
11	^1J(C1,C2)	82.75	4.23	−10.18	76.92		^2J(C1,C3)	−0.99	−0.90	0.06	−1.84
	^1J(C2,C3)	43.94	0.92	−1.06	44.01		^3J(C1,C4)	8.65	2.00	0.54	11.19
	^2J(C1,C3)	2.04	0.04	−0.33	1.71	**19**	^1J(C1,C2)	58.88	1.17	−7.03	53.21
	^2J(C2,C4)	0.60	−0.01	−0.23	0.38		^2J(C1,C3)	−1.35	1.39	2.52	2.52
	^3J(C1,C4)	6.39	0.05	0.06	6.42		^3J(C1,C4)	1.03	−0.63	0.11	0.49
	^4J(C1,C5)	0.78	−0.04	0.09	0.76		^4J(C1,C5)	1.75	1.75	−0.55	2.95

to 1.7 Hz) and couplings over more than three bonds vanish; ^3J(C,C) remains non-zero because of a through-space mechanism transmitted by J^{FC}.

When a double bond is present between the coupled carbons, the SD and PSO contributions to ^1J(C,C) are non-negligible ($J^{SD} \approx$ 3.9–4.2 Hz; $J^{PSO} \approx −10.2$ Hz), although J^{FC} remains dominant; thus reproducing experiment requires inclusion of non-contact terms. For σ sp^3–sp^2 ^1J(C,C), the SD and PSO contributions are small (≈ 0.9 and $\approx −1$ Hz, respectively) and largely cancel. For couplings beyond one bond in this group, J^{SD} and J^{PSO} are negligible and observable values arise primarily from J^{FC}.

4.1.2.3 Compounds with conjugated double bonds. For compounds **14–19**, ^1J(C,C) remains the largest coupling and ^3J(C,C) is often the next largest. Unlike the previous two groups, couplings over more than three bonds can be detectable ($\approx −3.2$ to 4.2 Hz in the set studied).

4.1.2.4 Acyclic compounds with conjugated double bonds. In linear polyenes (**14–16**), ^1J(C,C) depends strongly on whether the bond is double (≈ 76 Hz) or σ sp^2–sp^2 (≈ 56–60 Hz) and remains nearly constant along a given conjugated chain. The Ramsey contributions to ^1J(C,C) in the presence of a double

bond are numerically close to those found in compounds with isolated double bonds. For σ sp²–sp² ¹J(C,C) in these polyenes, the J^{SD} and J^{PSO} contributions are ≈1.4–1.8 Hz and ≈−3.5 to −3.0 Hz, respectively, while J^{FC} ≈57.8–61.8 Hz. These values differ from σ sp²–sp³ cases, confirming that both J^{FC} and the non-contact terms depend on hybridization and on involvement in a conjugated π system.

In these acyclic conjugated systems, the PSO contribution to couplings beyond one bond is negligible or vanishes, whereas the SD contribution shows characteristic behavior. For ²J(C,C), J^{SD} values (≈−2.7 to −1.6 Hz) are often larger in absolute value than J^{FC} (≈0.5–1.6 Hz), so the total ²J(C,C) is controlled by J^{SD} when the two terms do not cancel. For ³J(C,C), J^{FC} increases (≈7.9–8.7 Hz) relative to saturated systems (≈5.9–6.4 Hz); J^{SD} for ³J(C,C) depends on the number of conjugated bonds in the pathway (≈3.5–3.8 Hz when two conjugated bonds lie in the path, ≈0.6–0.8 Hz when only one does).

For longer-range couplings, J^{SD} values tend to be larger when the coupling pathway is fully conjugated, e.g., ⁵J(C1,C6) > ⁴J(C1,C5). At the same time, J^{FC} generally decreases with distance (approaching ≈1 Hz for very long pathways), indicating that J^{FC} is relatively insensitive to extended conjugation while J^{SD} clearly reflects it. Our results show that for some long-range couplings with fully conjugated pathways, such as ⁵J(C1,C6) and ⁷J(C1,C8), the J^{SD} contribution exceeds J^{FC}. This finding contrasts with earlier work that considered only J^{FC}.[101]

4.1.2.5 Cyclic compounds with conjugated/alternated double bonds. Cyclooctatetraene (**17**) is non-planar and lacks extended π conjugation. Its ¹J(C,C) values are similar to those of linear analogues. For double bonds, the Ramsey terms are comparable to those in linear compounds, and for σ sp²–sp² bonds, J^{FC} is also similar. In contrast, J^{SD} and J^{PSO} decrease substantially for these bonds (by ≈50% and ≈30%, respectively) and nearly vanish for couplings over more than two bonds. This drastic reduction in J^{SD}, compared to linear conjugated systems, identifies it as a sensitive probe for the absence of extended conjugation in cyclic systems.

By contrast, compounds **18** and **19** are aromatic, planar, and possess fully delocalized π systems. Their high structural symmetry makes all bonds equivalent, which results in identical numerical values for all $^nJ(C,C)$ couplings of the same range n, as well as for their respective Ramsey terms ($^nJ^{FC}(C,C)$, $^nJ^{SD}(C,C)$, and $^nJ^{PSO}(C,C)$). However, these equal values arise from different physical origins: $^nJ^{FC}(C,C)$ is governed by the σ skeleton, whereas $^nJ^{SD}(C,C)$ and $^nJ^{PSO}(C,C)$ depend primarily on the π-electron distribution.

In benzene, the FC contributions to ¹J(C,C), ²J(C,C), and ³J(C,C) are 65, −1, and 8.6 Hz, respectively, while the PSO contributions are −7.23, 0, and 0.5 Hz. Although both J^{FC} and J^{PSO} reflect the variation in π character of the C–C bond relative to a localized double bond, their overall trends across these couplings resemble those of their linear analogues. In contrast, the SD contributions to ¹J(C,C), ²J(C,C), and ³J(C,C) are 1.4, −0.9, and 2.0 Hz, respectively. Remarkably, the SD contribution to ³J(C,C) exceeds that to ¹J(C,C), a trend opposite to that

observed in conjugated linear compounds for a ¹J(C,C) coupling across a double bond.

For compound **19**, the FC contribution to ¹J(C,C) is 58.9 Hz, while for longer-range couplings, J^{FC} values range between −1.3 and 1.7 Hz. The PSO contributions to ¹J(C,C) and ²J(C,C) are −7.0 and 2.5 Hz, respectively, becoming negligible beyond two bonds. Thus, as in benzene, the PSO term does not reveal extended conjugation. Conversely, the SD contributions to ¹J(C,C), ²J(C,C), ³J(C,C), and ⁴J(C,C) are 1.2, 1.4, −0.6, and 1.7 Hz, respectively. These results confirm the sensitivity of the SD term to extended conjugation and, moreover, suggest a π-electron delocalization that differs from that in benzene. In particular, the $^1J^{SD}(C,C)$ value is sensitive to the varying degrees of aromaticity in these systems.

Our results demonstrate that the J^{SD} term can detect cyclic delocalization and exhibits a characteristic pattern distinct from that in acyclic analogues. The SD term of J-couplings reliably reflects the presence and degree of extended π-delocalization, establishing it as the foundation for a new aromaticity index.

4.2 Definition of a novel aromaticity index

To optimize computational efficiency, we evaluated the performance of the cc-pVTZ basis set against ccJ-pVTZ for calculating the SD term of carbon–carbon J-couplings in the compounds shown in Fig. S1 (SI). As detailed in Table S3 (SI), the differences between the basis sets originate primarily from the FC term, as cc-pVTZ lacks the diffuse functions needed to accurately describe the wavefunction at the nucleus. In contrast, the SD and PSO terms show negligible variation.

A linear regression of $^nJ^{SD}(C,C)$ values obtained with cc-pVTZ and ccJ-pVTZ yields an R^2 = 0.9998, a slope of 0.904, and an intercept of 0.014 (Fig. S3, SI). This confirms that the cc-pVTZ basis set reliably reproduces the trends in SD term values obtained with ccJ-pVTZ. Therefore, in the remainder of this work, SD terms are calculated at the B3LYP/cc-pVTZ level, unless otherwise stated.

Regarding aromatic systems, two notable features of the SD term are the uniformity and magnitude of its values. For instance, the $^1J^{SD}(C,C)$ value in benzene is 1.27 Hz, compared to 1.08 Hz in the larger, less aromatic cyclooctatetraenyl dication.[16]

For couplings across more than one bond, however, orbital interactions within the π-system become more complex, making direct comparisons between systems of different ring sizes less straightforward. In contrast, for one-bond couplings, the SD contribution primarily reflects the π-system localized to the bond itself, a direct manifestation of the ring's overall delocalization. Since a key objective is to define an index applicable to both six-membered and other ring sizes, we base our new index on the SD term of the one-bond coupling constant. We define the spin-dipolar aromaticity index (SDAI) as follows:

$$SDAI = 1 - \frac{1}{b_{sd}}\sqrt{\frac{\sum_i^n \left(a_{sd} - {}^1J^{SD}(N,M)_i\right)^2}{n}} \quad (2)$$

22980 | *Phys. Chem. Chem. Phys.*, 2025, **27**, 22974–22989

This journal is © the Owner Societies 2025

In eqn (2), a_{sd} is a constant equal to the $^1J^{SD}(C,C)$ value in benzene (1.27 Hz), ensuring that SDAI = 1 for this archetypal aromatic system. The constant b_{sd} is chosen so that SDAI = 0 for cyclooctatetraene, a prototypical non-aromatic compound (b_{sd} = 1.77). The term $^1J^{SD}(N,M)_i$ represents the SD contribution to each of the n one-bond couplings, between the nuclei M and N, in an n-membered ring. This formulation allows direct comparison of aromaticity across systems with different sizes, while retaining
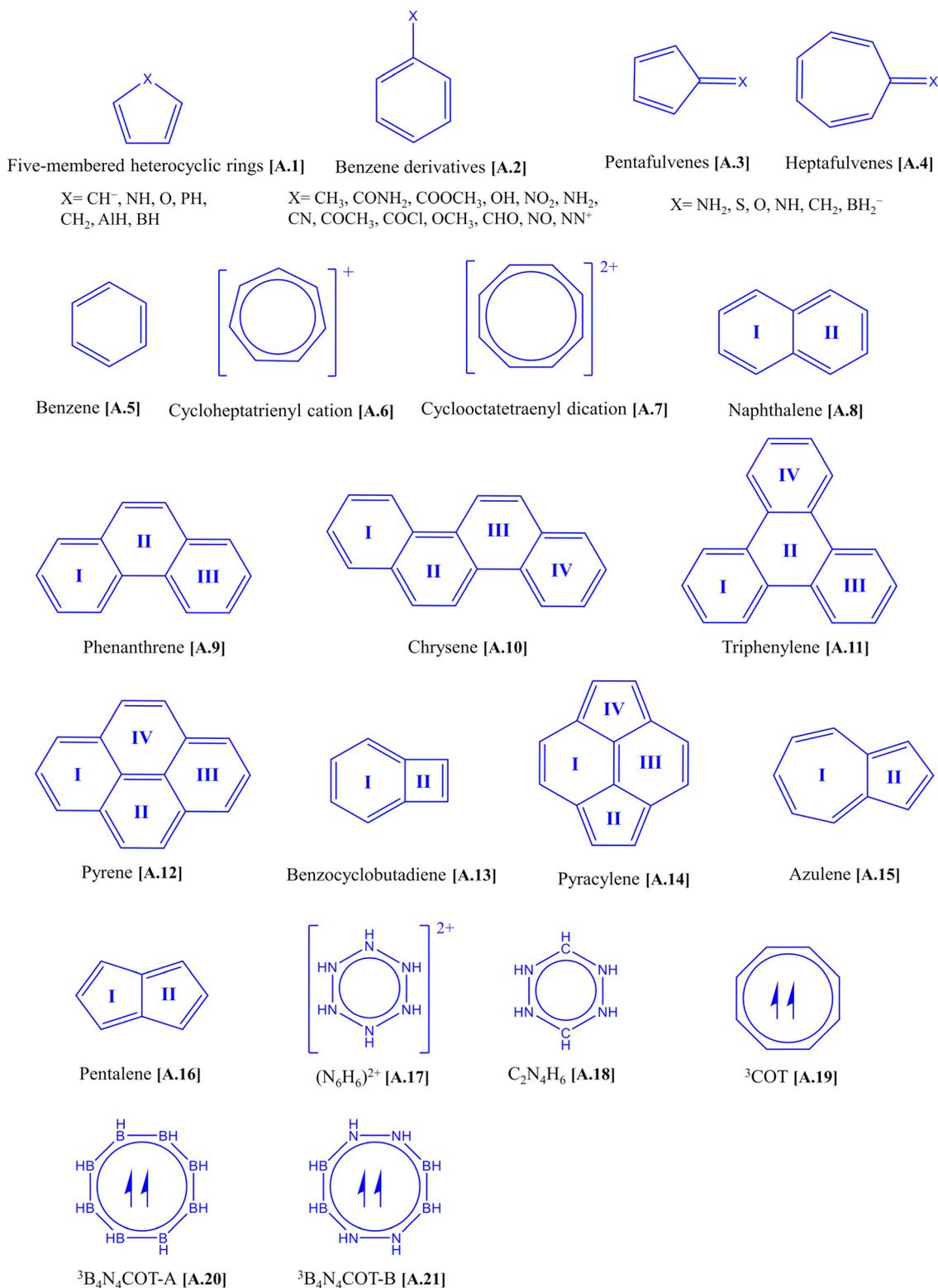

Fig. 3 Schematic structures of selected compounds used to evaluate the performance of SDAI as a new aromaticity index.

This journal is © the Owner Societies 2025

Phys. Chem. Chem. Phys., 2025, **27**, 22974–22989 | **22981**

benzene as reference point. As shown below, SDAI proves to be highly sensitive to variations in aromaticity.

4.3 Performance of SDAI as a new aromaticity index

In this section, we assess the reliability of the SDAI index for evaluating aromaticity in cyclic hydrocarbon and heterocyclic rings belonging to compounds previously classified as aromatic, nonaromatic, or antiaromatic. Our study includes five-membered heterocycles, mono-substituted benzene derivatives, substituted fulvenes and heptafulvenes, three 6π-electron hydrocarbon rings (to test ring-size dependence), and various polycyclic aromatic hydrocarbons comprising both benzenoid and non-benzenoid systems. We also analyze SDAI performance in compounds for which previous studies reported discrepancies between magnetic and electronic descriptors of aromaticity.[29,55] These compounds are shown in Fig. 3.

As noted earlier, SDAI takes benzene as the reference aromatic system, with a maximum value of 1. For less aromatic compounds, the SDAI value decreases. According to our results, systems with SDAI > 0.3 are classified as aromatic, while those with values < 0.3 are considered nonaromatic or antiaromatic. Within the aromatic group, compounds can be further distinguished as highly aromatic (0.75–1), moderately aromatic (0.45–0.75), or weakly aromatic (0.3–0.45).

We compared SDAI with other indices, including ASE, PDI, FLU, the Shannon Aromaticity (SA),[102] the multicenter index (MCI),[103] the normalized multicenter index (I_{NB}),[104] the normalized Giambiagi index (I_{NG}),[104] NICS(1)$_{zz}$, and HOMA. The more aromatic a system, the higher the ASE, PDI, MCI, I_{NB}, I_{NG}, and HOMA values, whereas the FLU and SA indices decrease. For NICS, more negative values correspond to stronger aromaticity. In cases where additional indices are used, we provide the relevant references for their interpretation.

4.3.1 Heterocyclic five-membered rings.
Table 2 shows the SDAI values for five-membered heterocycles (see Fig. 3). This representative series includes aromatic, non-aromatic, and antiaromatic species and is often used to test aromaticity indices. For comparison, ASE, SA, and NICS(1)$_{zz}$ values are also reported.

Rings with X = CH$^-$, NH, or O are aromatic with six π-electrons, though their aromaticity depends on the heteroatom. In the cyclopentadienyl anion (X = CH$^-$), the negative charge is symmetrically delocalized, giving five equivalent

bonds and making it the most aromatic species in the series. In pyrrole (X = NH) and furan (X = O), the heteroatom contributes a lone pair from a p-orbital to the π-system. Both overlap effectively with the carbon 2p-orbitals, but nitrogen donates more efficiently due to its lower electronegativity, so pyrrole is more aromatic than furan. Thus, the aromaticity order is CH$^-$ > NH > O.

Systems with X = CH$_2$ or PH are considered non-aromatic, while X = AlH or BH yield antiaromatic species. SDAI reproduces the expected order:

$$CH^- > NH > O > PH > CH_2 > AlH > BH$$

This order agrees with ASE, NICS(1)$_{zz}$, and SA values. These results show that SDAI reliably reflects changes in π-electron delocalization within heterocyclic five-membered rings.

4.3.2 Benzene derivatives.
Table 3 reports SDAI values for fourteen monosubstituted benzenes (see Fig. 3), along with FLU$^{1/2}$, PDI, and NICS(1)$_{zz}$. Previous studies indicate that substituents partially localize π-electrons and reduce symmetry, thereby lowering aromaticity. However, these effects are moderate and do not significantly alter the electronic structure of the benzene ring. An aromaticity index is reliable if it assigns the maximum value to benzene, lower but still aromatic values to its derivatives, and moderate differences relative to benzene.

As expected, SDAI assigns the maximum value (1.0) to unsubstituted benzene. Substituents reduce aromaticity to varying degrees. The NN$^+$ group has the strongest effect (SDAI = 0.861), consistent with other indices, as its electron-withdrawing and negative inductive effects synergistically reduce delocalization. Other strong electron-withdrawing groups, like NO, generally also induce large decreases. In contrast, substituents such as NH$_2$, which possess a strong electron-donating resonance effect that partially compensates for its inductive effect, cause a smaller reduction in aromaticity (SDAI = 0.973). Other groups with weaker electronic effects, like CH$_3$ and OH, yield SDAI values close to 1.0 (0.985 and 0.981, respectively), reflecting their minimal impact on π-electron delocalization.

Table 2 ASE, NICS(1)$_{zz}$ (ppm), SA and SDAI (in atomic units) values for selected five-membered heterocyclics rings. See Fig. 3

X	ASE^a	NICS(1)$_{zz}$^{b}	SA $\times 10^{2\,c}$	SDAI^d
CH$^-$	22.05	−34.32	2×10^{-7}	0.727
NH	20.57	−31.83	0.0958	0.438
O	14.77	−27.97	0.2543	0.330
PH	3.20	−14.04	0.3192	0.162
CH$_2$	0.00	−13.12	0.4919	0.120
AlH	−9.98	13.85	0.6785	−0.060
BH	−22.49	37.80	0.9053	−1.558

^{a} From ref. 26. ^{b} Calculated at B3LYP/aug-cc-pVTZ. ^{c} From ref. 102. ^{d} Calculated at B3LYP/cc-pVTZ.

Table 3 FLU$^{1/2}$, PDI (in atomic units), HOMA, NICS(1)$_{zz}$ (in ppm) and SDAI values for selected in mono-substituted benzene derivatives. See Fig. 3

X	FLU$^{1/2\,a}$	PDI^b	HOMA^a	NICS(1)$_{zz}$^{c}	SDAI^d
H	0.000	0.100	0.989	−29.80	1.000
CH$_3$	0.015	0.097	0.984	−28.29	0.985
CONH$_2$	0.021	0.096	0.984	−27.82	0.984
COOCH$_3$	0.023	0.095	0.983	−27.83	0.980
OH	0.039	0.093	0.989	−27.05	0.981
NO$_2$	0.029	0.093	0.994	−27.87	0.975
NH$_2$	0.040	0.091	0.976	−25.35	0.973
CN	0.031	0.094	0.977	−28.14	0.970
COCH$_3$	0.029	0.095	0.973	−27.66	0.967
COCl	0.030	0.093	0.978	−27.40	0.963
OCH3	0.044	0.092	0.981	−27.53	0.957
CHO	0.028	0.094	0.980	−27.75	0.951
NO	0.043	0.091	0.981	−26.27	0.922
NN$^+$	0.078	0.079	0.955	−25.29	0.861

^{a} From ref. 16. ^{b} Calculated at HF/cc-pVTZ. ^{c} Calculated at B3LYP/aug-cc-pVTZ. ^{d} Calculated at B3LYP/cc-pVTZ.

22982 | *Phys. Chem. Chem. Phys.*, 2025, **27**, 22974–22989

This journal is © the Owner Societies 2025

The trends obtained with SDAI are in line with those from the other indices listed in Table 3, fulfilling the reliability criterion mentioned above. HOMA follows these trends as well, except for NO_2, which shows a slightly higher value than benzene, although the difference is minimal (0.005).

These findings support SDAI as a reliable tool for assessing aromaticity in substituted benzenes and detecting subtle changes in electron delocalization. They also underscore the benzene π-system's resistance to substituent-induced perturbations, explaining its remarkable stability and central role in organic chemistry.

4.3.3 Penta and heptafulvenes. The substituted penta- and heptafulvenes analyzed here are shown in Fig. 3, and their calculated aromaticity indices (SDAI, HOMA, MCI, I_{NB}, and $NICS(1)_{zz}$) are presented in Table 4. The aromaticity of these rings is governed by the electronegativity of the π-bonded X-substituent, which determines the dominant zwitterionic resonance structure.[16]

For pentafulvenes, electron-donating substituents enhance aromaticity by stabilizing the 6-π electron form, while electron-withdrawing substituents reduce it by favoring the 4-π electron form. In contrast, in heptafulvenes electron-donating substituents reduce aromaticity by stabilizing the 8π form, whereas electron-withdrawing ones increase it by promoting the 6-π structure.

The SDAI values for the pentafulvenes indicate increasing aromaticity in the order: $NH_2^+ <$ O $<$ NH $<$ $CH_2 <$ BH_2^-. These results agree with the substituents' electronic properties: X = BH_2^- leads to aromatic character, X = CH_2 and NH to non-aromaticity, and X = O and NH_2^+ to antiaromaticity. The same order is obtained from the $NICS(1)_{zz}$, MCI, and I_{NB} indices. The HOMA index yields a nearly identical trend but swaps the order for X = NH_2^+ and X = O. Nonetheless, all indices agree in classifying these two compounds as antiaromatic. Thus, the proposed SDAI index successfully quantifies the aromaticity of both penta- and heptafulvenes.

4.3.4 Ring size dependence in 6π-electron systems. Previous studies have shown that reliable aromaticity descriptors

Table 5 HOMA, FLU$^{1/2}$, MCI, NICS(1)$_{zz}$ (in ppm), and SDAI values for compounds **A.5–A.7**. See Fig. 3

Compounds	HOMA^a	FLU$^{1/2a}$	MCI^a	NICS(1)$_{zz}$^{b}	SDAI^c
A.5	0.989	0.000	0.072	−29.80	1.000
A.6	0.984	0.023	0.057	−26.95	0.921
A.7	0.896	0.048	0.041	−25.71	0.891

^{a} From ref. 16. ^{b} Calculated at B3LYP/aug-ccpVTZ. ^{c} Calculated at B3LYP/cc-pVTZ.

reflect variations in aromaticity as ring size changes.[16] To verify that the SDAI meets this criterion, we analyzed three 6π-electron systems—C_6H_6, $C_7H_7^+$, and $C_8H_8^{2+}$ (**A.5–A.7** in Fig. 3)—for which aromaticity is known to decrease with increasing ring size.[16] The SDAI, as well as the HOMA, FLU$^{1/2}$, MCI, and NICS(1)$_{zz}$ values, are reported in Table 5. All descriptors yield the same aromaticity order: $C_6H_6 > C_7H_7^+ > C_8H_8^{2+}$. Thus, SDAI correctly reproduces the expected decrease in aromaticity as ring size increases in 6π-electron hydrocarbons.

4.3.5 Polycyclic aromatic hydrocarbons. The aromaticity of polycyclic aromatic hydrocarbons (PAHs) containing benzenoid and non-benzenoid rings has been widely investigated using various indices.[62,63,102,103,105,106] To assess the reliability of SDAI in describing these systems, we analyzed nine representative PAHs and included benzene for reference (Fig. 3). The corresponding HOMA, PDI, FLU and SDAI values are listed in Table 6.

In most cases, the SDAI agrees with the other indices in identifying the most aromatic ring within each system. As expected, SDAI indicates that naphthalene rings (**A.8**) are less aromatic than benzene. For PAHs with a single Clar structure (**A.9, A.11, A.12**), SDAI assigns higher aromaticity to rings with π-sextets, in accordance with Clar's rule. Thus, SDAI correctly shows that in phenanthrene (**A.9**), the outer rings are more aromatic than the inner one, while in pyrene (**A.12**) rings I and III are more aromatic than II and IV, a finding consistent with the other indices.

For triphenylene (**A.11**), SDAI yields values of 0.886 and 0.773 for the outer and inner rings, respectively, both within the aromatic range but showing the expected higher aromaticity of the outer rings. The deviations from benzene's aromaticity (0.114 and 0.228) indicate that the inner ring deviates twice as much as the outer ones, though both remain relatively small. SDAI also identifies the lateral rings (I, IV) of chrysene (**A.10**) as more aromatic than the inner ones (II, III), a finding consistent with the other indices.

In benzocyclobutadiene (**A.13**), SDAI and HOMA indicate moderate aromaticity for the six-membered ring, whereas PDI and FLU assign higher aromaticity. Additionally, the SDAI value of the four-membered ring (−0.833) indicates antiaromaticity, in line with the other indices.

For compound **A.14**, SDAI suggests moderate aromaticity for the six-membered rings, while HOMA, PDI, and FLU indicate stronger aromatic character. All indices agree on the non-antiaromatic nature of its five-membered rings.

Regarding azulene (compound **A.15**), the SDAI and FLU values indicate that the seven-membered ring is more aromatic

Table 4 HOMA, MCI, I_{NB}, NICS(1)$_{zz}$ (in ppm), and SDAI values for selected mono-substituted penta- and heptafulvenes. See Fig. 3

X	HOMA^a	MCI^a	I_{NB}^{a}	NICS(1)$_{zz}$^{b}	SDAI^c
Pentafulvenes					
NH_2^+	−0.83	−0.008	−0.0304	32.34	−1.531
O	−1.50	−0.002	−0.0231	13.45	−0.516
NH	−0.81	0.003	0.0258	4.67	−0.254
CH_2	−0.28	0.012	0.0330	−4.55	−0.014
BH_2^-	0.48	0.051	0.0441	−26.04	0.584
Heptafulvenes					
NH_2^+	0.80	0.036	0.0327	−15.04	0.643
O	0.27	0.018	0.0297	−6.25	0.379
NH	0.21	0.014	0.0286	4.77	0.192
CH_2	0.16	0.011	0.0275	19.29	−0.038
BH_2^-	0.02	0.003	0.0224	102.20	−1.339

^{a} From ref. 16. ^{b} Calculated at B3LYP/aug-cc-pVTZ. ^{c} Calculated at B3LYP/cc-pVTZ.

This journal is © the Owner Societies 2025

Phys. Chem. Chem. Phys., 2025, **27**, 22974–22989 | **22983**

Table 6 HOMA, PDI (in atomic units), FLU and SDAI values for selected polycyclic aromatic hydrocarbons. See Fig. 3

Compounds	Ring	HOMA[a]	PDI[b]	FLU[c]	SDAI[d]
A.5	I	0.981	0.100	0.000	1.000
A.8	I	0.769	0.073	0.009	0.741
A.9	I/III	0.854	0.081	0.005	0.837
	II	0.433	0.044	0.019	0.667
A.10	I/IV	0.804	0.078	0.008	0.806
	II/III	0.541	0.052	0.019	0.711
A.11	I/III/IV	0.889	0.085	0.003	0.886
	II	0.047	0.026	0.023	0.773
A.12	I/III	0.854	0.072	0.006	0.859
	II/IV	0.579	0.039	0.018	0.640
A.13	I	0.664	0.083	0.013	0.421
	II	−1.570		0.063	−0.833
A.14	I/III	0.755	0.067	0.010	0.589
	II/IV	−0.164		0.040	−0.037
A.15	I	0.515		0.010	0.705
	II	0.278		0.015	0.662
A.16	I	−0.381		0.046	−2.439

[a] Calculated at B3LYP/6-311++g(d,p) as implemented in the Multiwfn program. [b] Calculated at HF/cc-pVTZ. [c] From ref. 106, except **A.10** for ref. 63 and **A.16** for ref. 107. [d] Calculated at B3LYP/cc-pVTZ.

Table 7 NICS(1)$_{zz}$ (in ppm), $J(r)$ (in nA/T), I_{NG}, FLU and MCI for compound **A.5** and **A17–A21**. See Fig. 3

Compounds	NICS(1)$_{zz}$[ab]	$J(r)$[a]	$I_{NG} \times 10^{3f}$	FLU[bc]	MCI[bd]	SDAI[e]
A.5	−28.7	11.7	41.3	0.000	0.072	1.000
A.17	−25.7	10.1	11.9			−0.181
A.18	−25.5	10.3	11.4			0.058
A.19	−32.4			0.001	0.0275	0.671
A.20	−19.3			0.237	0.0016	0.272
A.21	−16.6	—		0.053	0.0013	−0.173

[a] From ref. 29. [b] From ref. 55. [c] From ref. 63. [d] From ref. 16. [e] Calculated at UB3LYP/cc-pVTZ. [f] I_{NG} values are reported multiplied by 10^3, following the convention of Zhao et al.[29]

than the five-membered one, both exhibiting significant aromatic character. In contrast, the HOMA index also identifies the seven-membered ring as the more aromatic ring but assigns it only a moderate aromatic character and an even smaller one to the five-membered ring.

Furthermore, the SDAI value calculated for the 10 π-electron perimeter of azulene (0.820) reveals that the external circuit is more aromatic than the individual five- and seven-membered rings, confirming the predominance of the 10 π-electron perimeter aromaticity recently reported by Dunlop et al.[108] For naphthalene, the SDAI value obtained for its 10 π-electron perimeter (0.737) is comparable to those of the individual six-membered rings, in good agreement with the findings of Bakouri et al.,[109] where EDDB analysis showed delocalization percentages of 46.8% for the perimeter and 41.3% for each ring.

Finally, the SDAI value for the five-membered rings of pentalene (**A.16**) indicates that it is a markedly antiaromatic compound, as expected. This result is also supported by the other aromaticity indices analyzed in this study.

4.3.6 Systems with discrepancies between magnetic and electronic aromaticity descriptors. This section evaluates the performance of the SDAI index on selected compounds (**A.17**, **A.18**, **A.20**, and **A.21** in Fig. 3), for which previous studies reported contradictory results between magnetic and electronic descriptors.[29,55] The SDAI values, together with indices from the literature, are presented in Table 7.

Frenking and co-workers[29] showed that the 10 π-electron planar systems $(N_6H_6)^{2+}$ (**A.17**) and $C_4N_2H_6$ (**A.18**) are not minima on their respective potential energy surfaces (PES), lying 82.0 and 115.5 kcal mol^{-1} above their most stable acyclic isomers. Nevertheless, magnetic descriptors—NICS(1)$_{zz}$ and current intensity $J(r)$, along with induced current density maps[29]—indicate that these species sustain a strong diamagnetic ring current comparable to that of benzene, suggesting a high degree of aromaticity. By contrast, the electron

delocalization index I_{NG} values for **A.5**, **A.17**, and **A.18** (41.3, 11.9, and 11.4, respectively) show that π-delocalization in $(N_6H_6)^{2+}$ and $C_4N_2H_6$ is much weaker than in benzene. The SDAI values of −0.181 and 0.058, respectively, further suggest that these systems are not aromatic, in agreement with the energetic and electronic criteria reported in ref. 29.

In a recent study, Ottosson and co-workers[55] compared the Baird aromaticity[110–113] of cyclooctatetraene (**A.19**) and its BN/CC isosteres B_4N_4COT-A (**A.20**) and B_4N_4COT-B (**A.21**) in their lowest triplet states (T_1). They found that in **A.20** and **A.21** the magnetic descriptors diverge from the electronic and energetic ones. At T_1, both isomers adopt highly symmetric and planar structures similar to **A.19**; however, $^3B_4N_4COT$-A is 128.7 kcal mol^{-1} lower in energy than $^3B_4N_4COT$-B.[55] The energetic aspects have been thoroughly discussed in ref. 55; here we simply note that they indicate ^3COT is clearly aromatic, whereas $^3B_4N_4COT$-A and $^3B_4N_4COT$-B are non-aromatic. Regarding the electronic aspect, Ottosson et al. employed the FLU and MCI indices, whose values are listed in Table 7. Both indices classify ^3COT as aromatic and the two isomers as non-aromatic. The SDAI values for ^3COT, $^3B_4N_4COT$-A, and $^3B_4N_4COT$-B are 0.671, 0.272, and −0.173, respectively, confirming that ^3COT is aromatic, while the two isosteres are non-aromatic. In agreement with energetic data and the MCI index, the SDAI values also reflect the lower stability of $^3B_4N_4COT$-B relative to $^3B_4N_4COT$-A.

This analysis shows that for molecules where traditional magnetic descriptors diverge from electronic and energetic ones, SDAI reproduces the trends predicted by the latter criteria.

5. Conclusions

In this work, we introduce a new aromaticity index based on the SD contribution to one-bond spin–spin coupling constants, designed to quantify local aromaticity in cyclic and polycyclic systems—the SDAI index. Beyond proposing an additional numerical descriptor, our goal was to reveal a physical manifestation of aromaticity by linking it to an objective NMR parameter—the J^{SD} term. This index demonstrates, for the first time, that aromaticity can be interpreted through a specific magnetic interaction: the coupling between nuclear magnetic moments mediated by delocalized π-electrons.

22984 | *Phys. Chem. Chem. Phys.*, 2025, **27**, 22974–22989

This journal is © the Owner Societies 2025

The SD term is computationally straightforward to evaluate. Using the B3LYP, B3P86, and PBE functionals in conjunction with the ccJ-pVTZ basis set, we achieved excellent agreement with experimental J-coupling values for C–C bonds of different hybridizations (sp^3–sp^3, sp^3–sp^2, and sp^2–sp^2). Moreover, calculations with the standard cc-pVTZ basis set reproduced the J^{SD} results obtained with the specialized ccJ-pVTZ and aug-cc-pVTZ sets, showing that SDAI can be efficiently computed with widely available quantum-chemical tools.

We examined the SD, PSO, and FC contributions to $^nJ(C,C)$, with n ranging from one to seven bonds, in both linear and cyclic compounds comprising saturated and unsaturated systems. We found that only the SD term reflects extended conjugation, showing distinctive value patterns that allow the detection of aromaticity. Our results show that in polyenes, long-range couplings such as $^5J(C1,C6)$ and $^7J(C1,C8)$ are dominated by the SD term, contrary to earlier studies that neglected this contribution.

We found that the SD contribution to $^1J(M,N)$ acts as a sensitive probe of the magnetic uniformity of the π-system, revealing how electrons transmit spin polarization between adjacent nuclei. In aromatic rings, this response is collective and uniform, yielding $^1J^{SD}(M,N)$ values close to those of benzene. In contrast, nonaromatic and antiaromatic systems display irregular spin polarization, producing large bond-to-bond variations in $^1J^{SD}(M,N)$, which may become negative, vanish, or exceed 4 Hz. A uniform spin-polarization pattern is therefore a necessary but not sufficient condition for aromaticity: when the resulting $^1J^{SD}(M,N)$ values differ significantly from those of benzene—as in the dication $[N_6H_6]^{2+}$—the system remains nonaromatic, even though it sustains diatropic ring currents. The SDAI index correctly classifies such systems as nonaromatic.

For a representative series of compounds—including five-membered heterocycles, mono-substituted benzenes, substituted fulvenes and heptafulvenes, and polycyclic hydrocarbons containing both benzenoid and non-benzenoid rings—we show that SDAI reproduces the aromaticity order obtained from established indices such as HOMA, NICS(1)$_{zz}$, PDI, and FLU. More importantly, in molecules where magnetic descriptors diverge from electronic and energetic ones, SDAI follows the trends of the latter, confirming its reliability as a physically grounded measure of aromaticity.

Unlike most traditional indices based on geometry, energy, or magnetic shielding, SDAI is founded on a physical basis that enables it to detect subtle variations in aromatic character, particularly in ambiguous systems where conventional descriptors may fail. Consequently, SDAI offers a new and complementary perspective that integrates the magnetic and electronic aspects of aromaticity into a single, accessible property.

Our findings demonstrate that the proposed index not only provides additional quantitative information but also deepens our understanding of aromaticity by unveiling a direct quantum-physical manifestation of this phenomenon—one that bridges nuclear magnetic interactions with the delocalized π-electron framework of aromatic systems.

Conflicts of interest

There are no conflicts of interest to declare.

Data availability

Acknowledgements

References

1 *Arene Chemistry: Reaction Mechanisms and Methods for Aromatic Compounds*, ed. J. Mortier, John Wiley & Sons, Hoboken, 2016.

2 A. F. Pozharskii, A. T. Soldatenkov and A. R. Katritzky, *Heterocycles in Life and Society: An Introduction to Heterocyclic Chemistry, Biochemistry and Applications*, John Wiley & Sons, Chichester, 2nd edn, 2011.

3 *Structure, Bonding and Reactivity of Heterocyclic Compounds*, ed. F. De Proft and P. Geerlings, Springer, Verlag Berlin Heidelberg, Heidelberg, 2014.

4 T. J. Ritchie and S. J. F. MacDonald, Physicochemical descriptors of aromatic character and their use in drug discovery, *J. Med. Chem.*, 2014, **57**, 7206–7215.

5 T. M. Krygowski, H. Szatylowicz, O. A. Stasyuk, J. Dominikowska and M. Palusiak, Aromaticity from the viewpoint of molecular geometry: Application to planar systems, *Chem. Rev.*, 2014, **114**, 6383–6422.

6 K. P. Vuayalakshmi and C. H. Suresh, Theoretical studies on the carcinogenicity of polycyclic aromatic hydrocarbons, *J. Comput. Chem.*, 2008, **29**, 1808–1817.

7 J. D. Hepworth, D. R. Waring and M. J. Waring, *Aromatic Chemistry*, The Royal Society of Chemistry, Cambridge, 2002.

8 Q. Li, Y. Zhang, Z. Xie, Y. Zhen, W. Hu and H. Dong, Polycyclic aromatic hydrocarbon-based organic semiconductors: ring-closing synthesis and optoelectronic properties, *J. Mater. Chem. C*, 2022, **10**, 2411–2430.

9 J. E. Anthony, Functionalized acenes and heteroacenes for organic electronics, *Chem. Rev.*, 2006, **106**, 5028–5048.

10 S. Kilaru, R. Gade, Y. Bhongiri, A. Tripathi, P. Chetti and S. Pola, Organic materials based on hetero polycyclic aromatic hydrocarbons for organic thin-film transistor applications, *Mater. Sci. Semicond. Process.*, 2022, **147**, 106730.

11 H. Szatylowicz, O. A. Stasyuk, M. Solà and T. M. Krygowski, Aromaticity of nucleic acid bases, *Wiley Interdiscip. Rev.: Comput. Mol. Sci.*, 2021, **11**, e1509.

12 Z. Badri and C. Foroutan-Nejad, Unification of ground-state aromaticity criteria – structure, electron delocalization, and energy – in light of the quantum chemical topology, *Phys. Chem. Chem. Phys.*, 2016, **18**, 11693–11699.

13 A. Stanger, NICS – Past and Present, *Eur. J. Org. Chem.*, 2020, 3120–3127.

14 R. Gershoni-Poranne and A. Stanger, Magnetic criteria of aromaticity, *Chem. Soc. Rev.*, 2015, **44**, 6597–6615.

15 F. Feixas, E. Matito, J. Poater and M. Solà, Quantifying aromaticity with electron delocalisation measures, *Chem. Soc. Rev.*, 2015, **44**, 6434–6451.

16 F. Feixas, E. Matito, J. Poater and M. Solà, On the performance of some aromaticity indices: a critical assessment using a test set, *J. Comput. Chem.*, 2008, **29**, 1543–1554.

17 Z. Chen, C. S. Wannere, C. Corminboeuf, R. Puchta and P. von R. Schleyer, Nucleus-Independent Chemical Shifts (NICS) as an Aromaticity Criterion, *Chem. Rev.*, 2005, **105**, 3842–3888.

18 M. K. Cyrański, Energetic aspects of cyclic pi-electron delocalization: Evaluation of the methods of estimating aromatic stabilization energies, *Chem. Rev.*, 2005, **105**, 3773–3811.

19 A. T. Balaban, D. C. Oniciu and A. R. Katritzky, Aromaticity as a cornerstone of heterocyclic chemistry, *Chem. Rev.*, 2004, **104**, 2777–2812.

20 M. Randić, Aromaticity of Polycyclic Conjugated Hydrocarbons, *Chem. Rev.*, 2003, **103**, 3449–3605.

21 P. Von Ragué Schleyer, Introduction: Aromaticity, *Chem. Rev.*, 2001, **101**, 1115–1117.

22 G. Merino, M. Solà, I. Fernández, C. Foroutan-Nejad, P. Lazzeretti, G. Frenking, H. L. Anderson, D. Sundholm, F. P. Cossío, M. A. Petrukhina, J. Wu, J. I. Wu and A. Restrepo, Aromaticity: Quo Vadis, *Chem. Sci.*, 2023, **14**, 5569–5576.

23 H. Ottosson, A focus on aromaticity: fuzzier than ever before?, *Chem. Sci.*, 2023, **14**, 5542–5544.

24 G. Frenking and A. Krapp, Unicorns in the world of chemical bonding models, *J. Comput. Chem.*, 2007, **28**, 15–24.

25 T. M. Krygowski and M. K. Cyrański, Structural Aspects of Aromaticity, *Chem. Rev.*, 2001, **101**, 1385–1419.

26 M. K. Cyrański, T. M. Krygowski, A. R. Katritzky and P. V. R. Schleyer, To what extent can aromaticity be defined uniquely?, *J. Org. Chem.*, 2002, **67**, 1333–1338.

27 A. R. Katritzky, M. Karelson, S. Sild, T. M. Krygowski and K. Jug, Aromaticity as a Quantitative Concept. 7. Aromaticity Reaffirmed as a Multidimensional Characteristic, *J. Org. Chem.*, 1998, **63**, 5228–5231.

28 P. J. Mayer and H. Ottosson, False Identification of (Anti)-aromaticity in Polycyclic Molecules in Ground and Excited States Through Incorrect Use of NICS, *J. Phys. Org. Chem.*, 2025, **38**, e70000.

29 L. Zhao, R. Grande-Aztatzi, C. Foroutan-Nejad, J. M. Ugalde and G. Frenking, Aromaticity, the Hückel 4*n* + 2 Rule and Magnetic Current, *ChemistrySelect*, 2017, **2**, 863–870.

30 R. C. Benson, C. L. Norris, W. H. Flygare and P. Beak, A Classification of 2- and 4-Pyrone as Nonaromatic on the Basis of Molecular Magnetic Suscepttbility Anisotropies, *J. Am. Chem. Soc.*, 1971, **93**, 5591–5593.

31 W. H. Flygare, Magnetic interactions in molecules and an analysis of molecular electronic charge distribution from magnetic parameters, *Chem. Rev.*, 1974, **74**, 653–687.

32 D. H. Sutter and W. H. Flygare, Molecular g Values, Magnetic Suscepttbility Anisotropies, Second Moment of the Charge Distribution, and Molecular Quadrupole Moments in Ethylenimine and Pyrrole, *J. Am. Chem. Soc.*, 1969, **91**, 6895–6902.

33 H. J. Dauben, J. D. Wilson and J. L. Laity, Diamagnetic Susceptibility Exaltation as a Criterion of Aromaticity, *J. Am. Chem. Soc.*, 1968, **90**, 811–813.

34 H. J. Dauben, J. D. Wilson and J. L. Laity, Diamagnetic Susceptibility Exaltation in Hydrocarbons, *J. Am. Chem. Soc.*, 1969, **91**, 1991–1998.

35 F. De Proft and P. Geerlings, Conceptual and computational DFT in the study of aromaticity, *Chem. Rev.*, 2001, **101**, 1451–1464.

36 R. H. Mitchell, Measuring Aromaticity by NMR, *Chem. Rev.*, 2001, **101**, 1301–1316.

37 R. V. Williams, W. D. Edwards, P. Zhang, D. J. Berg and R. H. Mitchell, Experimental verification of the homoaromaticity of 1,3,5-cycloheptatriene and evaluation of the aromaticity of tropone and the tropylium cation by use of the dimethyldihydropyrene probe, *J. Am. Chem. Soc.*, 2012, **134**, 16742–16752.

38 C. Foroutan-Nejad, Interatomic Magnetizability: A QTAIM-Based Approach toward Deciphering Magnetic Aromaticity, *J. Phys. Chem. A*, 2011, **115**, 12555–12560.

39 S. Coriani, P. Lazzeretti, M. Malagoli and R. Zanasi, On CHF calculations of second-order magnetic properties using the method of continuous transformation of origin of the current density, *Theor. Chim. Acta*, 1994, **89**, 181–192.

40 P. Lazzeretti, M. Malagoli and R. Zanasi, Computational approach to molecular magnetic properties by continuous transformation of the origin of the current density, *Chem. Phys. Lett.*, 1994, **220**, 299–304.

41 A. Ghosh, S. Larsen, J. Conradie and C. Foroutan-Nejad, Local versus global aromaticity in azuliporphyrin and benziporphyrin derivatives, *Org. Biomol. Chem.*, 2018, **16**, 7964–7970.

42 R. Zanasi, Coupled Hartree–Fock calculations of molecular magnetic properties annihilating the transverse paramagnetic current density, *J. Chem. Phys.*, 1996, **105**, 1460–1469.

43 E. Steiner and P. W. Fowler, Patterns of ring currents in conjugated molecules: a few-electron model based on orbital contributions, *J. Phys. Chem. A*, 2001, **105**, 9553–9562.

44 P. Lazzeretti, Assessment of aromaticity via molecular response properties, *Phys. Chem. Chem. Phys.*, 2004, **6**, 217–223.

45 D. Geuenich, K. Hess, F. Köhler and R. Herges, Anisotropy of the induced current density (ACID), a general method to

22986 | *Phys. Chem. Chem. Phys.*, 2025, **27**, 22974–22989

This journal is © the Owner Societies 2025

quantify and visualize electronic delocalization, *Chem. Rev.*, 2005, **105**, 3758–3772.

46 J. Jusélius, D. Sundholm and J. Gauss, Calculation of current densities using gauge-including atomic orbitals, *J. Chem. Phys.*, 2004, **121**, 3952–3963.

47 H. Fliegl, S. Taubert, O. Lehtonen and D. Sundholm, The gauge including magnetically induced current method, *Phys. Chem. Chem. Phys.*, 2011, **13**, 20500–20518.

48 D. Sundholm, H. Fliegl and R. J. F. Berger, Calculations of magnetically induced current densities: theory and applications, *Wiley Interdiscip. Rev.: Comput. Mol. Sci.*, 2016, **6**, 639–678.

49 S. Pathak, R. Bast and K. Ruud, Multiconfigurational Self-Consistent Field Calculations of the Magnetically Induced Current Density Using Gauge-Including Atomic Orbitals, *J. Chem. Theory Comput.*, 2013, **9**, 2189–2198.

50 E. Paenurk and R. Gershoni-Poranne, Simple and efficient visualization of aromaticity: bond currents calculated from NICS values, *Phys. Chem. Chem. Phys.*, 2022, **24**, 8631–8644.

51 P. Bultinck, S. Fias and R. Ponec, Local Aromaticity in Polycyclic Aromatic Hydrocarbons: Electron Delocalization versus Magnetic Indices, *Chem. – Eur. J.*, 2006, 8813–8818.

52 Y. C. Lin, D. Sundholm and J. Jusélius, On the Aromaticity of the Planar Hydrogen-Bonded (HF)3 Trimer, *J. Chem. Theory Comput.*, 2006, **2**, 761–764.

53 Z. Badri, S. Pathak, H. Fliegl, P. Rashidi-Ranjbar, R. Bast, R. Marek, C. Foroutan-Nejad and K. Ruud, All-Metal Aromaticity: Revisiting the Ring Current Model among Transition Metal Clusters, *J. Chem. Theory Comput.*, 2013, **9**, 4789–4796.

54 C. Foroutan-Nejad, Is NICS a reliable aromaticity index for transition metal clusters?, *Theor. Chem. Acc.*, 2015, **134**, 1–9.

55 P. Preethalayam, N. Proos Vedin, S. Radenković and H. Ottosson, Azaboracyclooctatetraenes reveal that the different aspects of triplet state Baird-aromaticity are nothing but different, *J. Phys. Org. Chem.*, 2023, **36**, e4455.

56 C. Foroutan-Nejad, Magnetic Antiaromaticity---Paratropicity—Does Not Necessarily Imply Instability, *J. Org. Chem.*, 2023, **88**, 14831–14835.

57 T. Janda and C. Foroutan-Nejad, Why is Benzene Unique? Screening Magnetic Properties of C$_6$H$_6$ Isomers, *ChemPhysChem*, 2018, **19**, 2357–2363.

58 S. Shaik, A. Shurki, D. Danovich and P. C. Hiberty, A Different Story of π-DelocalizationThe Distortivity of π-Electrons and Its Chemical Manifestations, *Chem. Rev.*, 2001, **101**, 1501–1539.

59 J. P. Malrieu, M. Giequel, P. W. Fowler, C. Lepetit, J. L. Heully and R. Chauvin, Direct Evaluation of Cyclic Contributions to the π Energy of Conjugated Hydrocarbons from Strongly Localized Zero-Order Pictures†, *J. Phys. Chem. A*, 2008, **112**, 13203–13214.

60 C. Angeli and J. P. Malrieu, Aromaticity: an ab Initio Evaluation of the Properly Cyclic Delocalization Energy and the π-Delocalization Energy Distortivity of Benzene, *J. Phys. Chem. A*, 2008, **112**, 11481–11486.

61 J. Jara-Cortés and J. Hernández-Trujillo, Energetic Analysis of Conjugated Hydrocarbons Using the Interacting Quantum Atoms Method, *J. Comput. Chem.*, 2018, **39**, 1103–1111.

62 J. Poater, X. Fradera, M. Duran and M. Solà, The delocalization index as an electronic aromaticity criterion: Application to a series of planar polycyclic aromatic hydrocarbons, *Chem. – Eur. J.*, 2003, **9**, 400–406.

63 E. Matito, M. Duran and M. Solà, The aromatic fluctuation index (FLU): a new aromaticity index based on electron delocalization, *J. Chem. Phys.*, 2005, **122**, 014109.

64 D. W. Szczepanik, M. Andrzejak, J. Dominikowska, B. Pawełek, T. M. Krygowski, H. Szatylowicz and M. Solà, The electron density of delocalized bonds (EDDB) applied for quantifying aromaticity, *Phys. Chem. Chem. Phys.*, 2017, **19**, 28970–28981.

65 M. Máximo-Canadas, R. S. S. Oliveira, M. A. S. Oliveira and I. Borges, A New Set of Aromaticity Descriptors Based on the Electron Density Employing the Distributed Multipole Analysis (DMA), *ACS Omega*, 2025, **10**, 14157–14175.

66 H. Günther, *NMR Spectroscopy. Basic Principles, Concepts, and Applications in Chemistry*, Wiley-VCH, Weinheim, Germany, 3rd edn, 2013.

67 T. Helgaker, M. Jaszunski and K. Ruud, Ab Initio Methods for the Calculation of NMR Shielding and Indirect Spin − Spin Coupling Constants, *Chem. Rev.*, 1999, **99**, 293–352.

68 *Calculation of NMR and EPR Parameters. Theory and Applications*, ed. M. Kaupp, M. Bühl and G. Malkin Vladimir, Wiley-VCH, Weinheim, 2004.

69 T. Helgaker, M. Jaszuński and M. Pecul, *The quantum-chemical calculation of NMR indirect spin–spin coupling constants*, 2008.

70 L. B. Krivdin, Carbon–carbon spin–spin coupling constants: practical applications of theoretical calculations, *Prog. Nucl. Magn. Reson. Spectrosc.*, 2018, **105**, 54–99.

71 N. F. Ramsey, Electron coupled interactions between nuclear spins in molecules, *Phys. Rev.*, 1953, **91**, 303–307.

72 J. Gräfenstein and D. Cremer, Analysis of the paramagnetic spin–orbit transmission mechanism for NMR spin–spin coupling constants using the paramagnetic spin–orbit density distribution, *Chem. Phys. Lett.*, 2004, **383**, 332–342.

73 J. Gräfenstein and D. Cremer, Analysis of the spin–dipole transmission mechanism for NMR spin–spin coupling constants using orbital contributions, spin polarization, and spin–dipole energy density distribution, *Chem. Phys. Lett.*, 2004, **387**, 415–427.

74 D. Cremer, E. Kraka, A. Wu and W. Lüttke, Can One Assess theπ Character of a C–C Bond with the Help of the NMR Spin–Spin Coupling Constants?, *ChemPhysChem*, 2004, **5**, 349–366.

75 P. F. Provasi, G. A. Aucar and S. P. A. Sauer, Large long-range F–F indirect spin-spin coupling constants. Prediction of measurable F–F couplings over a few nanometers, *J. Phys. Chem. A*, 2004, **108**, 5393–5398.

76 J. Gräfenstein and D. Cremer, Unusual long-range spin–spin coupling in fluorinated polyenes: a mechanistic analysis, *J. Chem. Phys.*, 2007, **127**, 174704.

This journal is © the Owner Societies 2025

Phys. Chem. Chem. Phys., 2025, **27**, 22974–22989 | **22987**

77 M. N. C. Zarycz, M. A. Schiel, E. Angelina and R. D. Enriz, Covalence and π-electron delocalization influence on hydrogen bonds in proton transfer process of o-hydroxy aryl Schiff bases: a combined NMR and QTAIM analysis, *J. Chem. Phys.*, 2021, **155**, 054307.

78 M. Randić, Aromaticity Revisited, *Adv. Quantum Chem.*, 2018, **77**, 167–199.

79 J. Olsen and P. Jørgensen, Linear and nonlinear response functions for an exact state and for an MCSCF state, *J. Chem. Phys.*, 1985, **82**, 3235–3264.

80 O. Vahtras, H. Ågren, P. Jørgensen, H. J. A. Jensen, S. B. Padkjær and T. Helgaker, Indirect nuclear spin–spin coupling constants from multiconfiguration linear response theory, *J. Chem. Phys.*, 1992, **96**, 6120–6125.

81 M. A. Watson, P. Sałek, P. Macak, M. Jaszuński and T. Helgaker, The calculation of indirect nuclear spin–spin coupling constants in large molecules, *Chem. – Eur. J.*, 2004, **10**, 4627–4639.

82 W. Kohn and L. J. Sham, Self-consistent equations including exchange and correlation effects, *Phys. Rev.*, 1965, **140**, 1133–1138.

83 M. J. Frisch, G. W. Trucks, H. B. Schlegel, G. E. Scuseria, M. A. Robb, J. R. Cheeseman, G. Scalmani, V. Barone, B. Mennucci, G. A. Petersson, H. Nakatsuji, M. Caricato, X. Li, H. P. Hratchian, A. F. Izmaylov, J. Bloino, G. Zheng, J. L. Sonnenberg, M. Hada, M. Ehara, K. Toyota, R. Fukuda, J. Hasegawa, M. Ishida, T. Nakajima, Y. Honda, O. Kitao, H. Nakai, T. Vreven, J. A. Montgomery, Jr., J. E. Peralta, F. Ogliaro, M. Bearpark, J. J. Heyd, E. Brothers, K. N. Kudin, V. N. Staroverov, R. Kobayashi, J. Normand, K. Raghavachari, A. Rendell, J. C. Burant, S. S. Iyengar, J. Tomasi, M. Cossi, N. Rega, N. J. Millam, M. Klene, J. E. Knox, J. B. Cross, V. Bakken, C. Adamo, J. Jaramillo, R. Gomperts, R. E. Stratmann, O. Yazyev, A. J. Austin, R. Cammi, C. Pomelli, J. W. Ochterski, R. L. Martin, K. Morokuma, V. G. Zakrzewski, G. A. Voth, P. Salvador, J. J. Dannenberg, S. Dapprich, A. D. Daniels, Ö. Farkas, J. B. Foresman, J. V. Ortiz, J. Cioslowski and D. J. Fox, *Gaussian 16 Revision C.01*, Gaussian, Inc., Wallingford CT, 2016.

84 C. Lee, W. Yang and R. G. Parr, Development of the Colle-Salvetti correlation-energy formula into a functional of the electron density, *Phys. Rev. B: Condens. Matter Mater. Phys.*, 1988, **37**, 785–789.

85 S. Grimme, J. Antony, S. Ehrlich and H. Krieg, A consistent and accurate ab initio parametrization of density functional dispersion correction (DFT-D) for the 94 elements H-Pu, *J. Chem. Phys.*, 2010, **132**, 154104.

86 S. Grimme, S. Ehrlich and L. Goerigk, Effect of the Damping Function in Dispersion Corrected Density Functional Theory, *J. Comput. Chem.*, 2011, **32**, 1456–1465.

87 R. Krishnan, J. S. Binkley, R. Seeger and J. A. Pople, Self-consistent molecular orbital methods. XX. A basis set for correlated wave functions, *J. Chem. Phys.*, 1980, **72**, 650–654.

88 A. D. Becke, Density-functional thermochemistry. III. The role of exact exchange, *J. Chem. Phys.*, 1993, **98**, 5648–5652.

89 J. P. Perdew, K. Burke and M. Ernzerhof, Generalized Gradient Approximation Made Simple, *Phys. Rev. Lett.*, 1996, **77**, 3865–3868.

90 J. P. Perdew, Density-functional approximation for the correlation energy of the inhomogeneous electron gas, *Phys. Rev. B: Condens. Matter Mater. Phys.*, 1986, **33**, 8822–8824.

91 P. F. Provasi, G. A. Aucar and S. P. A. Sauer, The effect of lone pairs and electronegativity on the indirect nuclear spin–spin coupling constants in CH$_2$X (X = CH$_2$, NH, O, S): Ab initio calculations using optimized contracted basis sets, *J. Chem. Phys.*, 2001, **115**, 1324–1334.

92 U. Benedikt, A. A. Auer and F. Jensen, Optimization of augmentation functions for correlated calculations of spin-spin coupling constants and related properties, *J. Chem. Phys.*, 2008, **129**, 064111.

93 T. H. Dunning Jr, Gaussian basis sets for use in correlated molecular calculations. I. The atoms boron through neon and hydrogen, *J. Chem. Phys.*, 1989, **90**, 1007–1023.

94 K. Wolinski, J. F. Hinton and P. Pulay, Efficient Implementation of the Gauge-Independent Atomic Orbital Method for NMR Chemical Shift Calculations, *J. Am. Chem. Soc.*, 1990, **112**, 8251–8260.

95 J. R. Cheeseman, G. W. Trucks, T. A. Keith and M. J. Frisch, A comparison of models for calculating nuclear magnetic resonance shielding tensors, *J. Chem. Phys.*, 1996, **104**, 5497–5509.

96 R. F. W. Bader, *Atoms in Molecules A Quantum Theory*, Oxford University Press, Oxford, 1994.

97 T. Lu and F. Chen, Multiwfn: a multifunctional wavefunction analyzer, *J. Comput. Chem.*, 2012, **33**, 580–592.

98 K. Kamieńska-Trela and J. Wójcik, *High Resolution NMR Spectroscopy: Understanding Molecules and their Electronic Structures*, Elsevier, Oxford, 2013, pp. 347–424.

99 R. Suardíaz, C. Pérez, R. Crespo-Otero, J. M. G. De La Vega and J. S. Fabián, Influence of density functionals and basis sets on one-bond carbon-carbon NMR spin-spin coupling constants, *J. Chem. Theory Comput.*, 2008, **4**, 448–456.

100 H. Kjr, S. P. A. Sauer and J. Kongsted, Benchmarking NMR indirect nuclear spin-spin coupling constants: SOPPA, SOPPA(CC2), and SOPPA(CCSD) versus CCSD, *J. Chem. Phys.*, 2010, **133**, 144106.

101 J. Gräfenstein, T. Tuttle and D. Cremer, Analysis of long-range NMR spin–spin coupling in polyenes and the π-mechanism, *Phys. Chem. Chem. Phys.*, 2005, **7**, 452–462.

102 S. Noorizadeh and E. Shakerzadeh, Shannon entropy as a new measure of aromaticity, Shannon aromaticity, *Phys. Chem. Chem. Phys.*, 2010, **12**, 4742–4749.

103 P. Bultinck, R. Ponec and S. Van Damme, Multicenter bond indices as a new measure of aromaticity in polycyclic aromatic hydrocarbons, *J. Phys. Org. Chem.*, 2005, **18**, 706–718.

104 J. Cioslowski, E. Matito and M. Solà, Properties of Aromaticity Indices Based on the One-Electron Density Matrix, *J. Phys. Chem. A*, 2007, **111**, 6521–6525.

105 M. Giambiagi, M. Segre De Giambiagi, C. D. Dos Santos Silva and A. Paiva De Figueiredo, Multicenter bond indices

22988 | *Phys. Chem. Chem. Phys.*, 2025, **27**, 22974–22989

This journal is © the Owner Societies 2025

as a measure of aromaticity, *Phys. Chem. Chem. Phys.*, 2000, **2**, 3381–3392.

106 J. Dominikowska and M. Palusiak, EL: the new aromaticity measure based on one-electron density function, *Struct. Chem.*, 2012, **23**, 1173–1183.

107 K. P. Sudhakaran, A. Benny, A. T. John and M. Hariharan, Exploring the influence of graphene on antiaromaticity of pentalene, *Phys. Chem. Chem. Phys.*, 2023, **25**, 26986–26990.

108 D. Dunlop, L. Ludvíková, A. Banerjee, H. Ottosson and T. Slanina, Excited-state (anti) aromaticity explains why azulene disobeys Kasha's rule, *J. Am. Chem. Soc.*, 2023, **145**, 21569–21575.

109 O. El Bakouri, D. W. Szczepanik, K. Jorner, R. Ayub, P. Bultinck, M. Solà and H. Ottosson, Three-Dimensional Fully π-Conjugated Macrocycles: When 3D-Aromatic and When 2D-Aromatic-in-3D?, *J. Am. Chem. Soc.*, 2022, **144**, 8560–8575.

110 N. C. Baird, Quantum organic photochemistry. II. Resonance and aromaticity in the lowest 3.pi···pi.* state of cyclic hydrocarbons, *J. Am. Chem. Soc.*, 1972, **94**, 4941–4948.

111 H. Ottosson, Exciting excited-state aromaticity, *Nat. Chem.*, 2012, **4**, 969–971.

112 M. Rosenberg, C. Dahlstrand, K. Kilså and H. Ottosson, Excited State Aromaticity and Antiaromaticity: Opportunities for Photophysical and Photochemical Rationalizations, *Chem. Rev.*, 2014, **114**, 5379–5425.

113 J. Yan, T. Slanina, J. Bergman and H. Ottosson, Photochemistry Driven by Excited-State Aromaticity Gain or Antiaromaticity Relief, *Chem. – Eur. J.*, 2023, **29**, e202203748.

This journal is © the Owner Societies 2025

Phys. Chem. Chem. Phys., 2025, **27**, 22974–22989 | **22989**